Journal of Mining and Environment (JME), Vol. 15, No. 2, 2024, 557-579

Shahrood University of Technology

Journal of Mining and Environment (JME)

Journal homepage: www.jme.shahroodut.ac.ir

Iranian Society of Mining Engineering (IRSME)

Outlining of High-quality Parts of Coal by Concentration–Volume Fractal Model in North Kochakali Coal Deposit, Central Iran

Mojtaba Bazargani Golshan[1], Mehran Arian[1]*, Peyman Afzal[2], Lili Daneshvar Saein[3], and Mohsen Aleali[1]

1. Department of Earth Sciences., Science and Research Branch, Islamic Azad University, Tehran, Iran
2. Department of Petroleum and Mining Engineering., South Tehran Branch, Islamic Azad University, Tehran, Iran
3. Department of Geology., Payame Noor University, Tehran, Iran

Article Info

Received 7 August 2023

Received in Revised form 24 October 2023

Accepted 2 November 2023

Published online 2 November 2023

DOI: 10.22044/jme.2023.13446.2482

Keywords

Concentration-volume (C-V) fractal model

Coal

North Kochakali

Logratio matrix

Central Iran

Abstract

The aim is to use the Concentration-Volume (C-V) fractal model to identify high-quality parts of coal seams based on sulfur and ash concentrations. In the K1 and K7 coal seams in the North Kochakali coal deposit, 5 and 6 different populations of ash and sulfur content were obtained based on the results. According to this model, sulfur and ash concentrations below 1.81% and 33.1% for the K7 seam, and below 4.46% and 37.1% for the K1 seam, respective base on Russian standard for ash and high sulfur content of North Kochakali coals were considered as appropriate values. In order to identify the high-quality parts of K1 and K7 coal seams, plans at different depths were used based on the C-V fractal model. Plans at different depths suggests that the southern part of the K1 seam and the northern part of the K7 seam have the highest-quality based on sulfur and ash concentrations, which should be considered in the extraction operation. The logratio matrix was used to compare the results of the C-V fractal model with the geological data of pyrite veins and coal ash. This matrix indicates that sulfur content above 3.8% for the K7 seam and above 4.41% for the K1 seam have good and very good correlation with pyritic veins of geological data, respectively. There are good overall accuracy (OA) values in the correlation between parts of the seam with ash concentration above 37.1% and 45.7% for the K1 and K7 seams, respectively, and the coal ash obtained from the geological data.

1. Introduction

The North Kochakali coal deposit is located in the Tabas coal field; the coal deposits in North Kochakali are located in the Hojedk Formation. From the tectonic point of view, the Central Iran was a back-arc basin [1-7] related to the Neotethian subduction regime [8-15], and the Hojedk coal Formation was deposited there during the Late Triassic-to Jurassic [16]. The high thickness of the rocks of this time compared to the rocks after that shows the significant performance of the normal faults of the basin floor, which caused an increase in subsidence in the considered time. During Paleogene, intrusive igneous masses are injected into the thinned crust of back-arc basin, and the sulfur-bearing fluids associated with them penetrate into the coal bearing units through the normal faults of the basin floor [17]. During Neogene to Quaternary (closing of the back-arc basin due to the collision of the Arabian-Cimmerian plates), the normal faults mechanism was changed to strike-slip and reverse faults due to the change of extensional regime to the recent compressional position. This situation has caused the uplift and outcropping of the Hojedk formation.

Coal is an extraordinarily complex and heterogeneous material whose physical and chemical properties are relatively difficult to determine and usually contains a significant quantity of different organic and inorganic impurities that could cause environmental problems in its usage cycle [18-23]. According to the uses of coal, this material is divided into two categories: thermal coal and coke. Power plants are the main use of thermal coal. Considering the high

Corresponding author: mehranarian@yahoo.com (M. Arian)

sulfur and ash content in thermal coal and the uses of this type of coal, identifying the high-quality parts of the coal seams based on sulfur, and ash content plays a significant role in reducing environmental effects [24]. Various geological factors such as tectonics provide the basis for the upward of sulfur-containing fluids and lead to an increase sulfur concentration in the parts of the coal seams. Also, the faulting could be effective in the ash content, and in general, the quality of a coal seam. Misidentification of high-quality parts of the coal seams and extraction from these parts, as well as disregarding tectonic factors, lead to increased environmental effects and increased side costs.

Quality is an essential factor concerning the usefulness of coal deposits. Sulfur and ash are significant elements regarding coal quality. Sulfur is one of the harmful substances of coal. It is found in both organic and inorganic forms in coal [24, 25]. Pyrite is the primary inorganic sulfur impurity in the majority of coals [25, 26]. After coal combustion, large amounts of sulfur dioxide and carbon dioxide are released and affect the environment [27, 28].

Coal ash in thermal coal is one of the most burning issues in thermal power stations. This massive ash deposits in addition to environmental effects cover boiler pipes and other surfaces, and eventually cause equipment failure [29]. However, due to the high availability of this type of coal and the low mining cost, it is still used worldwide.

Coal plays a significant role in Iran's economy. Due to the increased price of oil and other energy carriers, coal can be a new energy source, and Iran is going to use thermal coal deposits as new energy sources; the first Iranian coal power plant is going to be established in central Iran, at Tabas coalfield [30].

The fractal model was first introduced by [31], and since the 1980s, this model has been widely used in geosciences in order to analyze spatial distribution of geo-chemical data and describe the mineralization zones from the host rock [32-45]. The concentration–area (C–A) and concentration–perimeter (C–P) fractal models were proposed by [32, 46] for estimation of elemental threshold values for various geochemical data [47]. Fractal modeling has been developed to detect different frequencies based on natural features, so different models have been presented in the branches of earth sciences such as number–size (N–S) by [31], power spectrum–area (S–A) by [48], concentration–distance (C–D) by [37], concentration–volume (C–V) by [40], and concentration–number (C–N) by [49-51], also the S-A and C-A fractal models to delineate environmental anomalies by [52].

[40] drew a logarithmic graph of concentration-volume; wherever the slope of the curve has changed drastically, the statistical population has changed. That indicates a sharp change in concentration and a function of changing geological and mineralization conditions [38, 53-59].

Fractal dimensions in geological, geo-physical, and geo-chemical processes correspond to variations in physical features such as lithology, mineralogy, vein and veinlets density or orientation, fluid phases, alteration zones, structural features and so on [60, 50]. For example, [61] used multi-fractal modeling of geological and geo-physical characteristics in Cu deposit, and [62] separated U and Th anomalies by radiometric geo-physical data with fractal method. Various geological mechanism such as petrogenesis, tectonic, metamorphism, and mineralization might be the origin of fractal characteristics. Such geological processes can lead to an increase or decrease in the concentration of elements in a rock unit, and can also expand the fractal dimension [63]; so due to differences in fractal dimensions gained from analysis of related data, different geological mechanisms can be explained [41]. C-V fractal model is used to detect mineralization zones in different mines. In addition, the C-V model has been used to classify the frequency of different regional variables such as lithological features and environmental and economic parameters [64].

[47] use C-V fractal models to recognized high-quality parts of coal seams in Parvadeh coal deposit, and found very good correlation between USGS standard and C-V fractal models; they also illustrated different phases of carbonization in Parvadeh coking coal by the C-V fractal model. In this research work, by using sulfur and ash concentrations and its enclosed volume C-V fractal graphs were drawn for K1 and K7 seams, then by using 3D models and plans at different depths base on C-V fractal graph high quality parts of K1 and K7 seams were detected. Finally, the results of the C-V fractal models were compared with pyritic veins and ash coals, which were derived by geological modeling. Since the sulfur and ash content plays a significant role in the coal quality, knowing the high-quality parts of the target coal seams can lead to reducing the environmental effects and increasing the economic value of the coal seams.

2. Geological Setting

The 45,000 km^2 Tabas coalfield is located 80-200 km south and southwest of Tabas. The granites of Uzbekkoh and Bafgh were identified in the north and west of Tabas coalfield, respectively. Most of the detrital sediments in this field were produced by the erosion of intrusive masses such as Ozbak–Koh, Zarigan, and Saghand [65]. The geological and sedimentological evidence regarding shale, sandstone, silt, and carbonate rocks suggests that they were formed in a deltaic environment [66]. Based on geological-tectonic components, the northern part is divided into three coal-bearing areas, namely Parvadeh, Nayband, and Mazino. The ten coal areas identified in the Tabas coalfield include Mazino, Kochakali (North and South), Kamar-e Mehdi, Kalshur, Kalmard, Kalshane, Dastgaran, Pirhajat, Jafaran, and Behabad.

In South Khorasan Province, the North Kochakali region is located about 75 km south of Tabas County. Structurally and geologically, this exploration zone is located to the north of the Tabas block.

Kalmard-Chahsorb or Kalshaneh is the only main and large fault that passes through the west of the zone with a northeastern-southwestern trend. It separates the embayment of Tabas-Shirgasht from the uplifting of Kalmard [67].

Studies show that in North Kochaklali, overall structure in the outcrop area is somewhat folded with extreme faults. Folding and faulting have produced two main synclines in Baghmshah and Parvadeh Formations, two main anticlines in Abhaji and Badamu Formations, and number of surface anticlines-synclines in Hojedk Formation. Generally, this region includes outcrops of the Jurassic Ab-haji, Badamu, Hojedk, Parvadeh, and Baghmshah Formations. In the west, the region is mostly covered by quaternary sediments. Middle Jurassic coal sediments in the North Kochakali region are located in the Hojedk Formation, which has deltaic facies with a series of sandstone sediments, green shales, coaly shales, and coal seams [68]. Badamu Formation with an average thickness of 30 meters (Toarcian-Bajocian) is located at the lower boundary of the Hojedk Formation, and its upper boundary in the North Kochakali is covered by the Mid-Upper Jurassic Parvadeh Formation with an average thickness of 12 meters [69]. A sinistral strike-slip fault with a northwest-southeast trend and revers component, a dextral strike-slip fault with a northeast-southeast trend and normal component, and a thrust fault have been identified in drilled borehole site with the northeast-southwest trend of area (North Kochakali) (Figures 1 and 2).

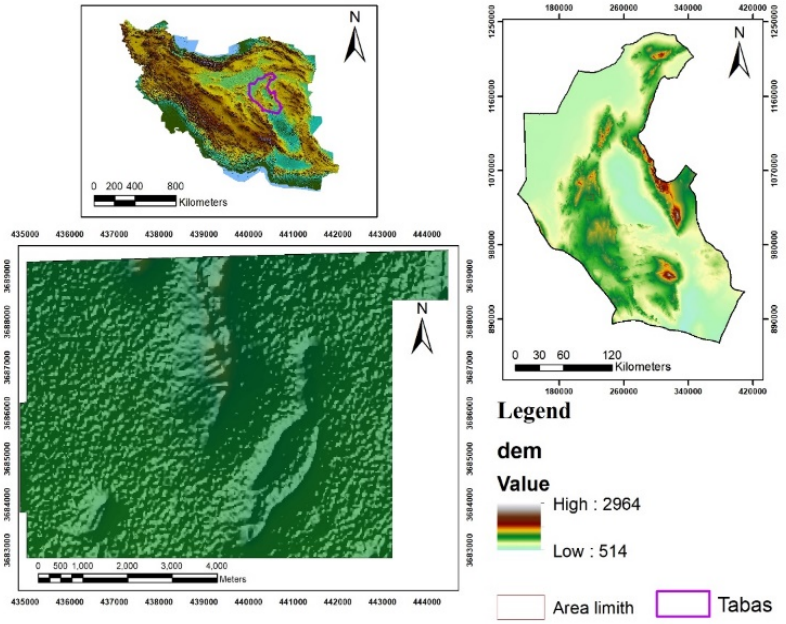

(a)

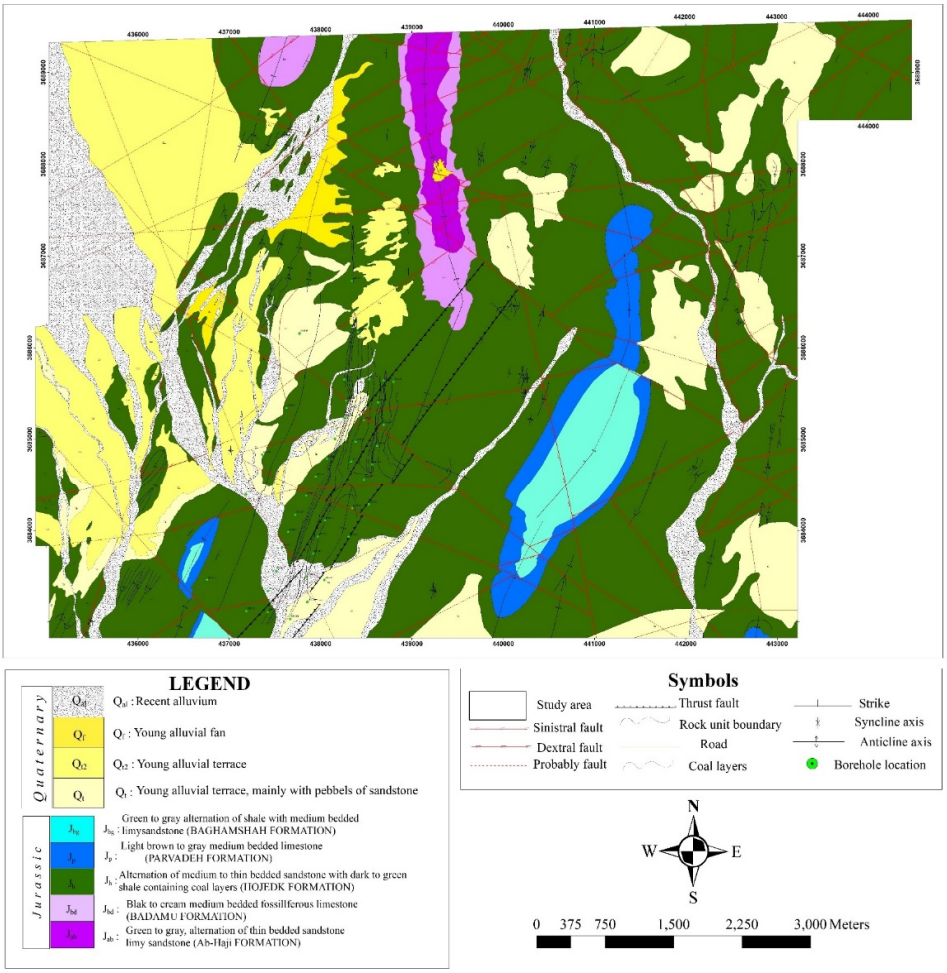

(b)

Figure 1. a- Geology setting (modified after [70]) b- Geology map of North Kochakali deposit (modified after [71]).

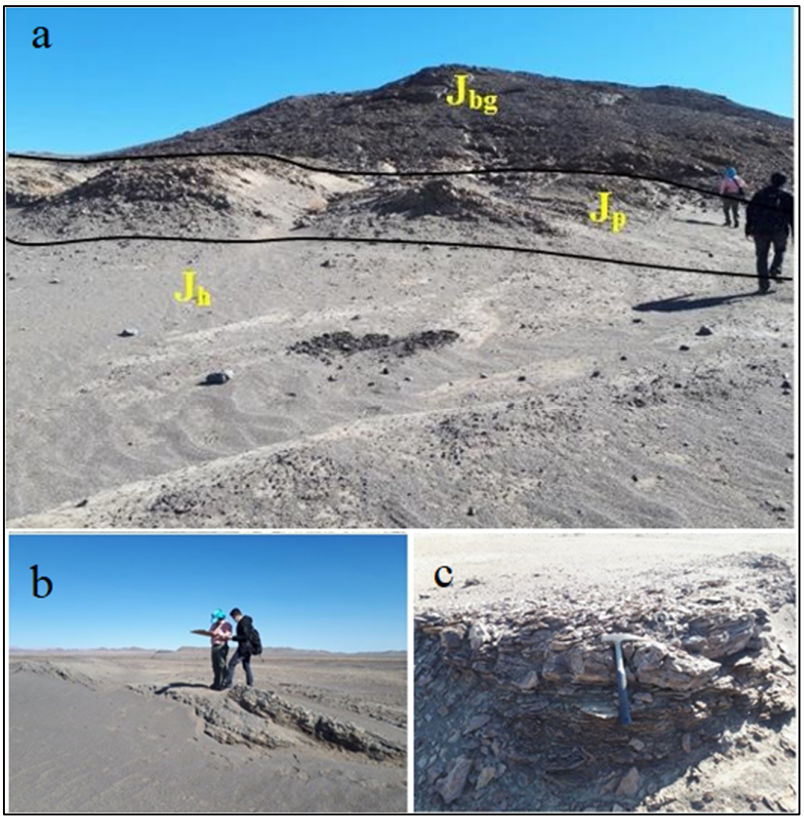

Figure 2. a- The boundary between the Hojedk, Parvadeh and Baghamshah Formations in the syncline structure in the southwest of the North Kochakali coal deposit b- Exposure of Hojedk Formation c- Coal seam in Hojedk Formation.

3. Methodology

The relationship between ore concentration and deposit volume or tonnages is the basis of using C-V fractal model [60, 49, 43, 44]. [40] suggested the Concentration–Volume fractal model for describing various porphyry-Cu mineralized zones from barren host rocks. The general form of this model is as follows:

$V(\rho \leq \upsilon) \propto \rho^{-a1}$; $V(\rho \geq \upsilon) \propto \rho^{-a2}$

In this model, V illustrate two volumes with concentration values lower than or equal to and more than ρ value; a and υ indicate the fractal dimensions and threshold values, respectively. The broken points in the straight sections fitted in the logarithmic graphs show the threshold values. Threshold values separating populations of different data values and in this model show boundaries between various mineralized zones. The volumes enclosed by a contour level ρ in a 3D model are used to calculate $V(\rho \leq \upsilon)$ and $V(\rho \geq \upsilon)$ [40].

In this study, first, 43 boreholes were excavated 200-500 meters apart, and then by using the geological information and the depth of the target seams in North Kochakali coal deposit, a 3D model of these seams was created by rock works 17 software. 15 target coal seams have been identified in North Kochakali, K1 is the deepest seam and K15 is the shallowest seam. According to the geometric features of the coal deposit, the region is 2,000 meters long, 3,720 meters wide, and 425 meters tall along the X, Y, and Z axes, then 50x50x.2 meters in the X, Y, and Z direction were assigned to any voxel dimensions (Figure 3).

K1 and K7 seams were selected for outlining of high-quality parts in this research works for this purpose 62 and 19 samples of sulfur, and ash from the K1 and K7 seams, respectively, were used for producing the two-seams 3D models in rockworks 17 based on sulfur and ash concentrations. After exporting data (concentrations of ash and sulfur) and sorting them in descending order and obtaining the cumulative frequency, the logarithmic data and cumulative frequency of ash and sulfur concentrations were used for plotting fractal graphs. Then by using sulfur and ash threshold values and enclosed volumes of these concentration different populations of ash and sulfur content base on C-V fractal graphs were obtained. Finally, K1 and K7 seams 3D modeling

of sulfur and ash concentrations models base on C-V fractal graph were drawn. In this research work, plots at different depths (750,800, 900,100, and 1100 meters) based on C-V fractal graphs were also used for checking the concentrations of sulfur and ash for determining the highest quality parts of the K1 and K7 seams.

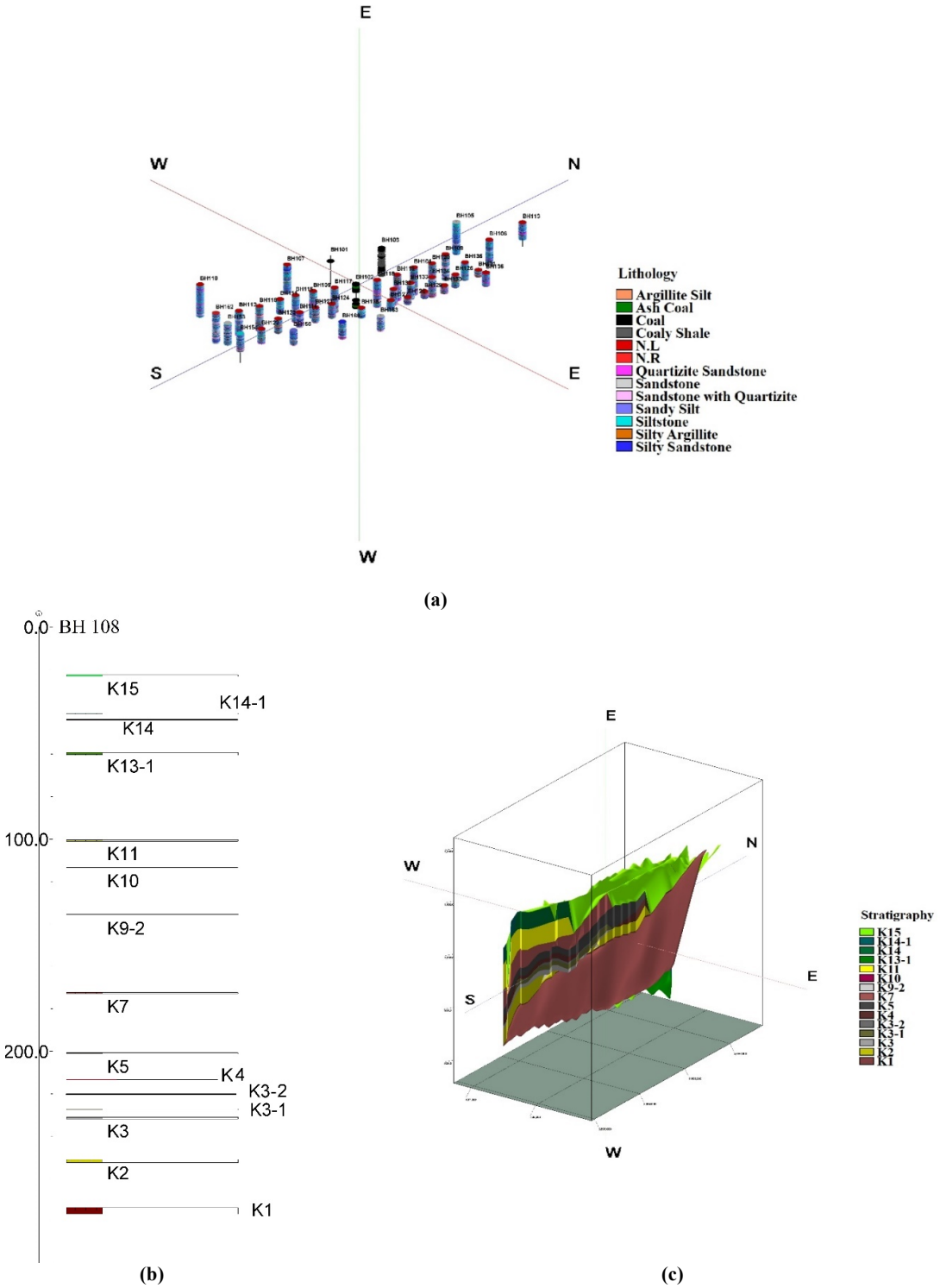

Figure 3. 3D model of boreholes site b- Target seams in BH 108 c- 3D model of North Kochakali coal seams (with exaggeration).

There are 2 standards to evaluate coal quality based on sulfur and ash concentrations Russian and USGS standard. In USGS standard, ash concentrations less than 15% are appropriate value but in Russian standard concentrations, less than 40% are considered as suitable values of ash. In both standards (Russian and USGS), sulfur concentrations more than 1.5% are considered as inappropriate values [72, 73] (Tables 1 and 2). In general, the threshold values of the Russian standard for ash content in coal are higher. Due to the thermal nature of North Kochakali coal and the high ash and sulfur content of this type of coal compared to coking coal, the Russian standard was used in this research work in order to check the results of the C-V fractal model.

Table 1. Coal classification based on USGS standard [72].

Category	Low	Moderate	high
Ash content	8 >	8-15	15 <
Sulfur content	1-1.5	1.5-2.5	2.5-3.5

Table 2. Coal classification based on Russian standard [73].

Category	Very low	Low	Moderate	Relatively high	High	Very high
Ash content	0-10	10-15	15-25	25-31	31-40	40 <
Sulfur content	0-1	1-1.5	1.5-2.5	2.5-3.5	3.5-5	5 <

4. Results and Discussion

The Logarithmic C-V graphs were made for sulfur and ash content in the K1 and K7 seams according to realization; one data could be used by accident as all realizations have same limit with an equal amount for maximum and minimum data [47] (Figures 4 and 5). Breakpoints between straight-line parts in the logarithmic graphs show threshold values for dividing of different sulfur and ash populations in K1 and K7 seams. According to the logarithmic C-V graph, the variable frequency of ash and sulfur for K7 seam were, respectively, 5 and 6, so different populations of ash and sulfur content for K7 seam were obtained (Tables 3 and 5) (Figure 5).

Due to the high sulfur content in North Kochakali coal, the lowest threshold values obtained from the C-V fractal graphs are selected as appropriate sulfur values, so population with very low sulfur content base on C-V fractal model (sulfur concentrations less than 1.86%) was selected as suitable sulfur concentration for K7 seam; this population is found in the northwest part of this seam. Ash concentrations less than 33.1% (population with low ash content) in K7 seam based on C-V fractal graph and Russian standard can be considered relatively good ash content, which are more common in the northern part of the K7 seam (Figure 6).

For the K1 seam, 5 and 6 different populations were obtained for ash and sulfur content, respectively (Tables 4 and 6) (Figure 4). According to the USGS standard, sulfur concentration more than 3.89% indicate pyritic veins in coal seams (Wood and Kehn, 1976). The high sulfur concentration (concentrations more than 3.89%) in the K1 seam indicates the presence of the pyrite vein in this seam. Sulfur concentrations less than 4.46 (population with very low sulfur content) based on C-V fractal graph are mostly found at south part of K1 seam. For ash in K1 seam low and moderate populations (concentration less than 37.1%) based on C-V fractal graph are known as the appropriate concentrations that correlate with Russian standard; these populations are found at the northern and parts of the southern of K1 seam (Figure 7).

Table 3. Different populations of sulfur content in K7 seam based on C–V fractal modeling.

Category	Very low	Low	Moderate	Relatively high	High	Very high
Sulfur content	1.81 >	1.81-2.75	2.75-3.38	3.38-3.8	3.8-4.16	4.16 <

Table 4. Different populations of sulfur content in K1 seam based on C–V fractal modeling.

Category	Very low	Low	Moderate	Relatively high	High	Very high
Sulfur content	< 4.46	4.46-6.45	6.45-6.9	6.9-7.4	7.4-7.9	7.9 <

Table 5. Different populations of ash content in K7 seam based on C–V fractal modeling.

Category	Low	Moderate	Relatively high	High	Very high
Ash content	< 33.1	33.1-45.7	45.7-66.06	66.06-85.1	85.1 <

Table 6. Different populations of ash content in K1 seam based on C–V fractal modeling.

Category	Low	Moderate	Relatively high	High	Very high
Ash content	< 30.2	30.2-37.1	37.1-50.11	50.11-72.4	72.4 <

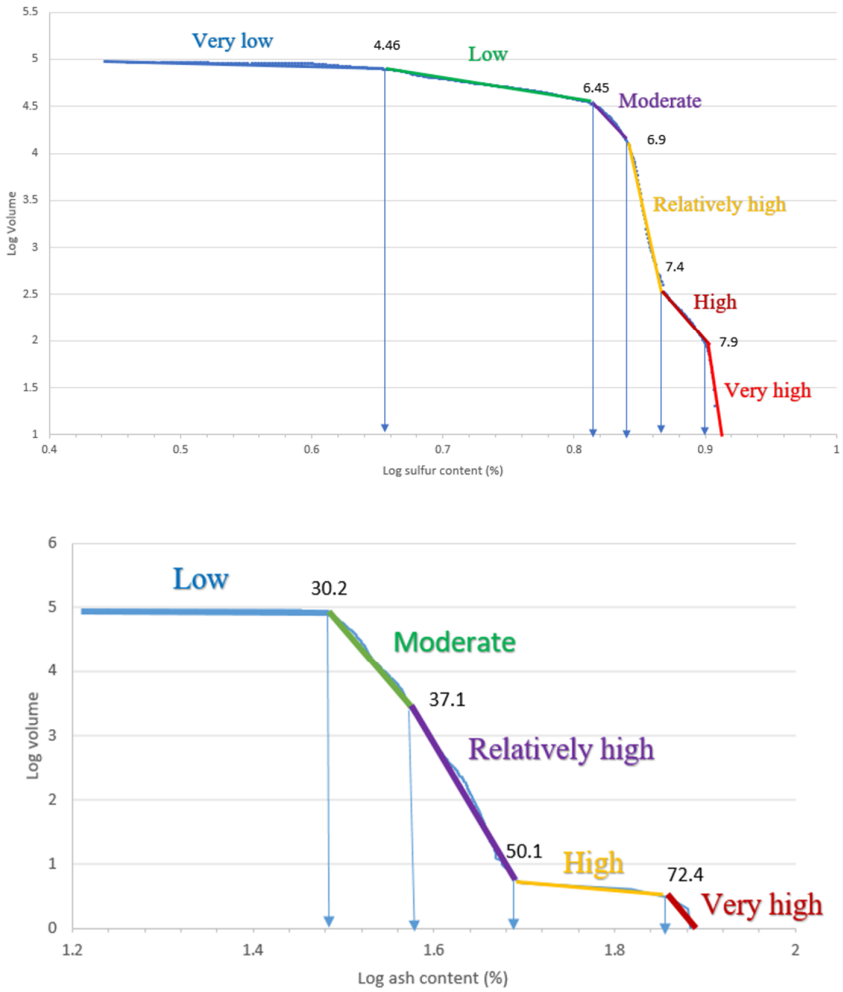

Figure 4. Logarithmic C–V graphs of sulfur and ash content for K1 seam in the North Kochakali deposit according to realization (colored lines show various populations).

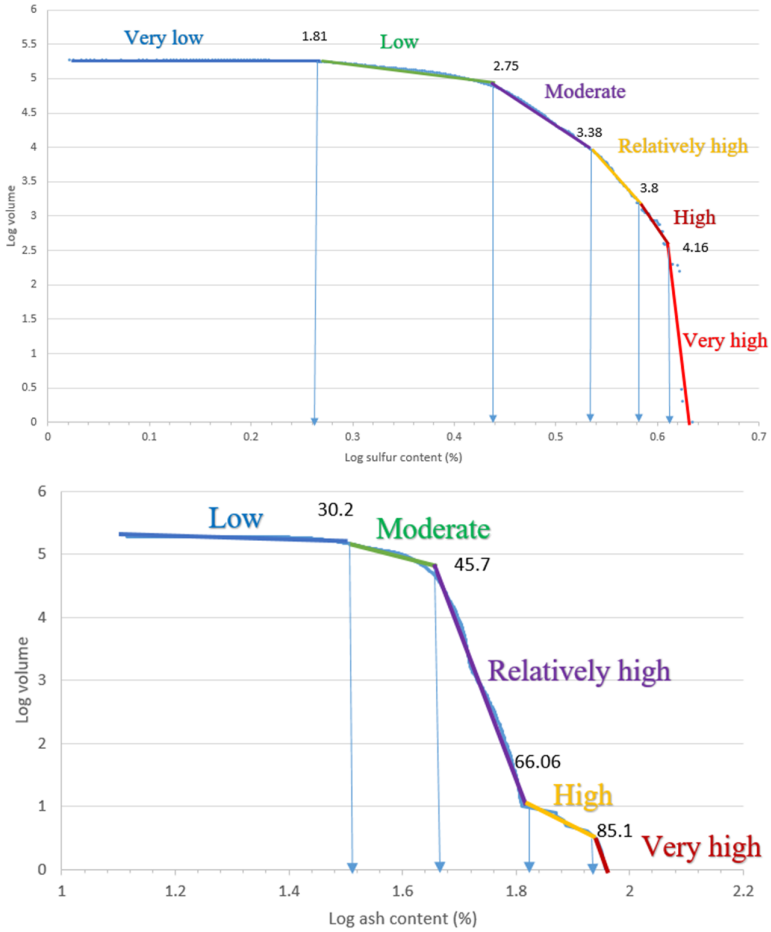

Figure 5. Logarithmic C–V graphs of sulfur and ash content for K7 seam in the North Kochakali deposit according to realization (colored lines show various populations).

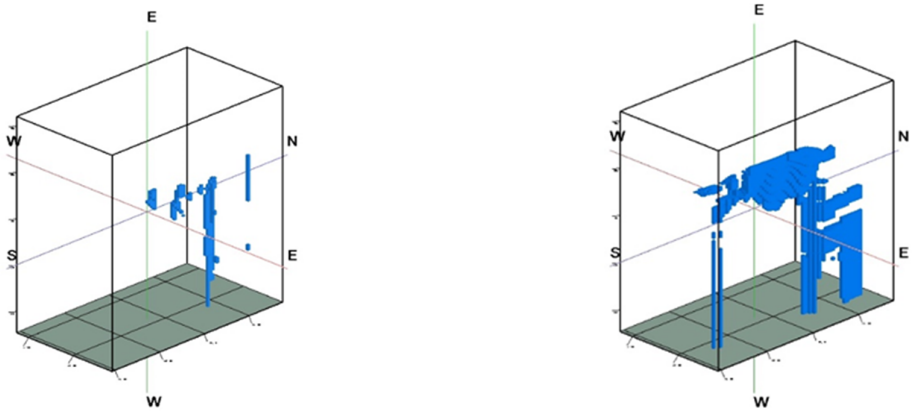

(a) **(b)**

Figure 6. a- Sulfur concentrations less than 1.81 b- ash concentrations less than 33.1 in K7 seam based on C–V fractal graphs.

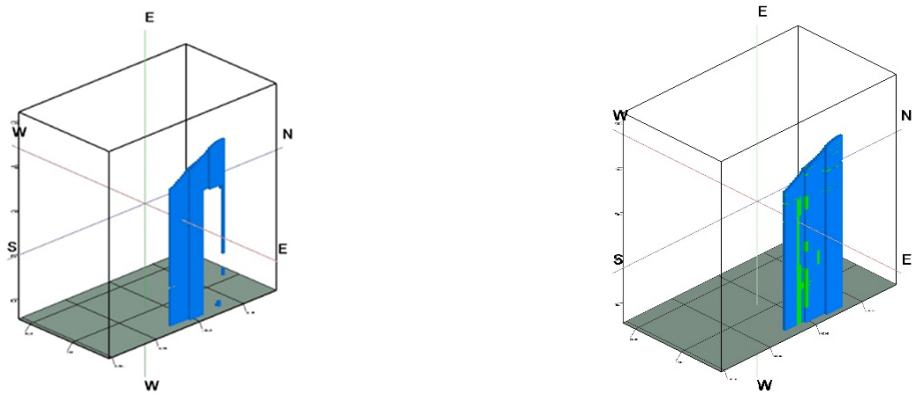

(a) (b)

Figure 7. a- Sulfur concentrations less than 4.41 b- ash concentrations less than 37.1 in K1 seam based on C–V fractal graphs.

Given the high sulfur concentrations in the K1 seam based on C-V fractal model, sulfur concentrations less than 4.46, which are considered low for this seam, are found at all depth (755, 800, 900, 1000, and 1100 meters) in the southern part (Figures 8, 9, and 10). Based on the C-V fractal model, the high and very high sulfur concentrations in the K1 seam are, respectively, within 7.4-7.9% and more than 7.9%. These sulfur concentrations in the K1 seam are concentrated at 755 and 800 meters of depth in the northern part (Figure 8). At 900 and 1000 meters of depth, high and very high sulfur concentrations at 755 and 800 meters of depth are transferred to the western part generally. At the depth of 900 and 1000 meters compared to the depth of 800 meters, the abundance of very high sulfur concentrations are slightly increased and these are more concentrated in the western part of the seam (Figure 9). Note the lack of high and very high sulfur concentration at 1100 meters of depth.

In K7, seam sulfur concentrations less than 1.81% (population with very low sulfur content) based on the C-V fractal model at 900 and 1000 meters of depth, these concentrations are found in the western part and in 1100-meter depth are recognizable in the north part of K7 seam (Figures 12 and 13). Low sulfur concentrations within 1.81%-2.75% in the K7 seam are found at 755 and 800 meters of depth in the northwest, at 900 meters of depth in the north and northwest, and at 1,100 meters of depth at the center and north part of the seam (Figures 11, 12, and 13). Sulfur concentrations more than 3.8 indicate the presence of the pyrite vein at 755, 800, 900, and 1000 meters of depth are located in the southeast of the seam. However, sulfur concentrations greater than 3.8% are less widespread at 1000 meters of depth and absent at 1100 meters of depth.

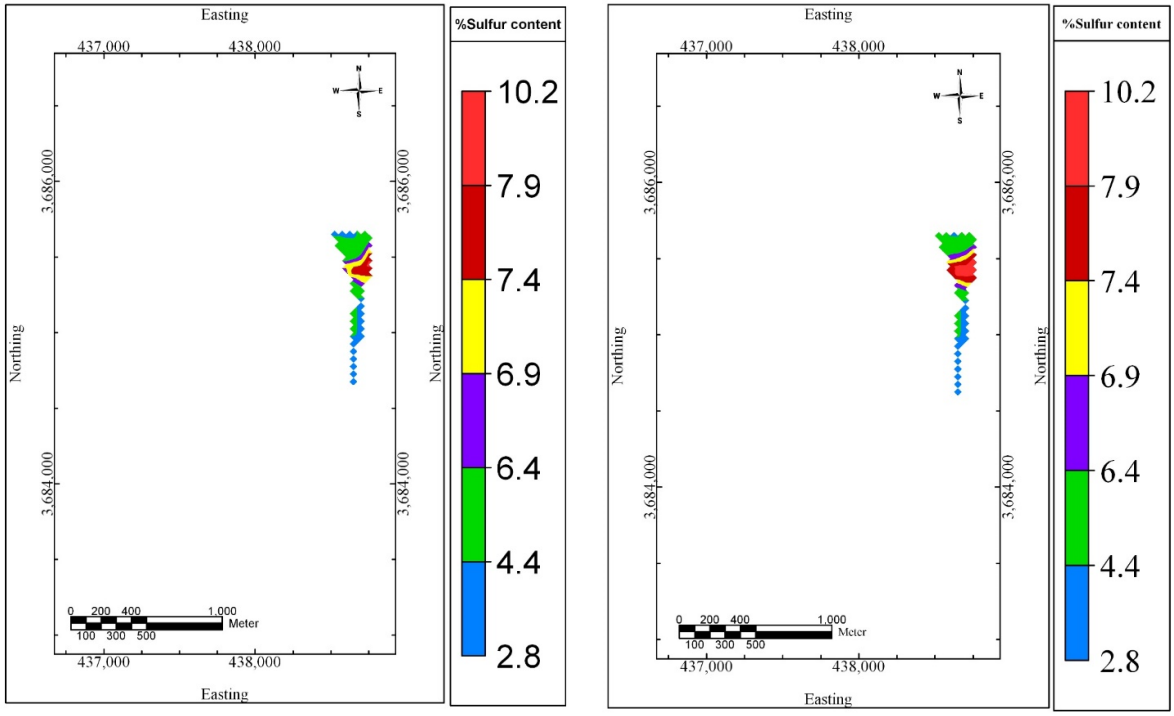

(a) **(b)**

Figure 8. Sulfur plan map in K1 seam (a- at 755 meters and b- at 800 meters).

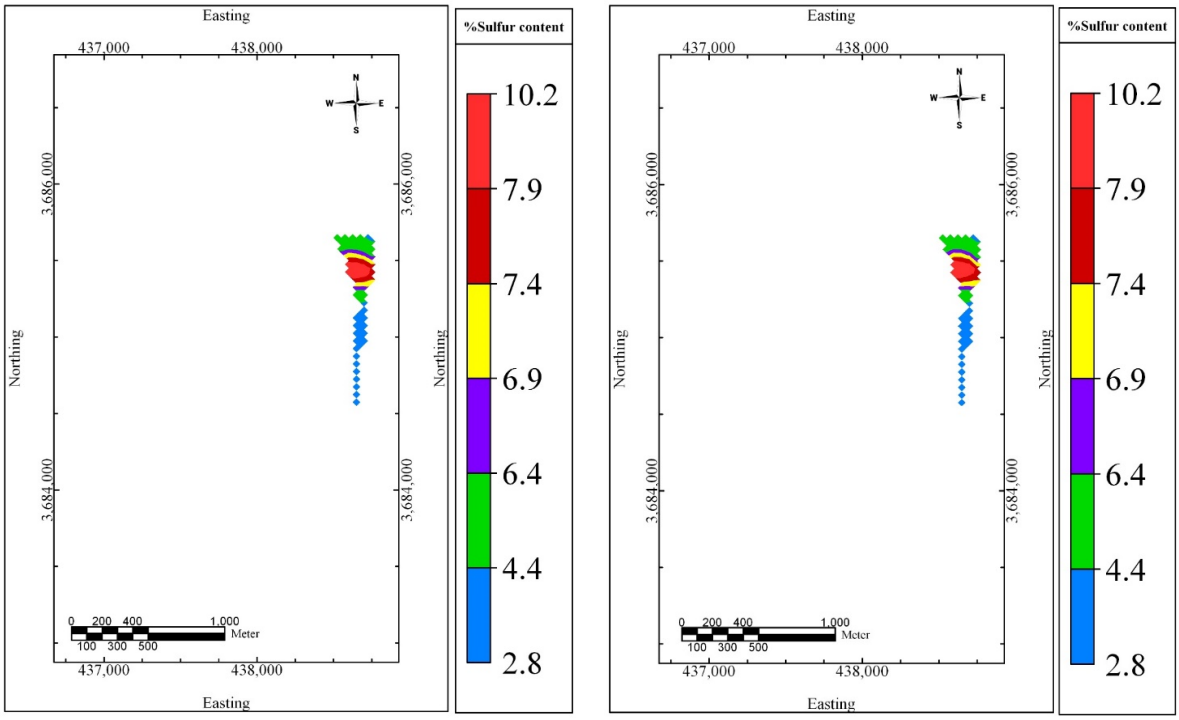

(c) **(d)**

Figure 9. Sulfur plan map in K1 seam (c- at 900 meters and d- at 1000 meters).

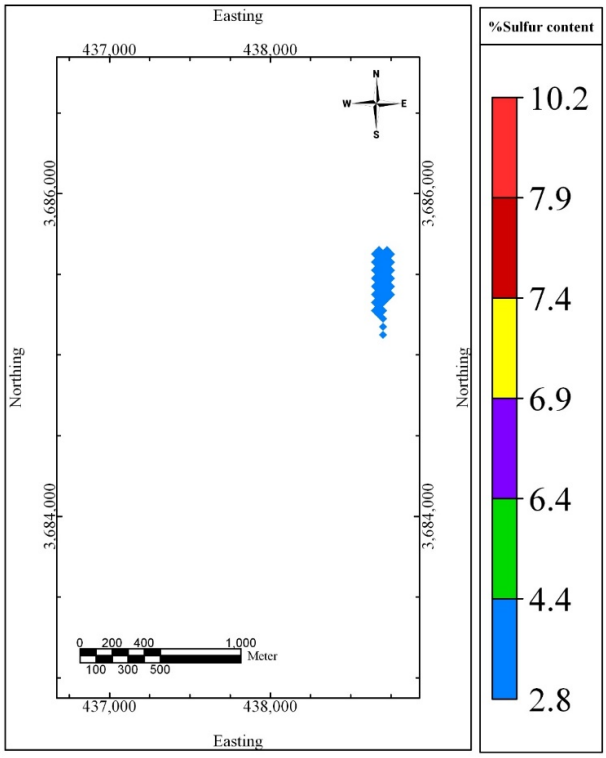

Figure 10. Sulfur plan map in K1 seam at 1100 meters.

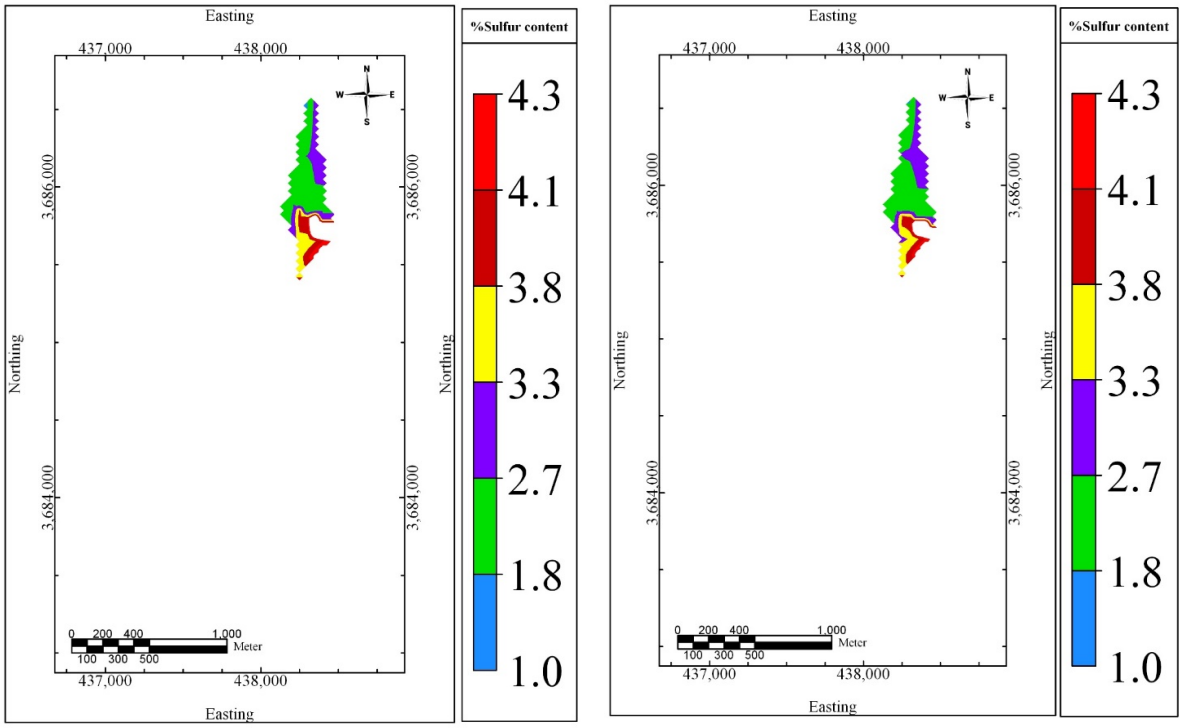

(a) **(b)**

Figure 11. Sulfur plan map in K7 seam (a- at 755 meters and b- at 800 meters).

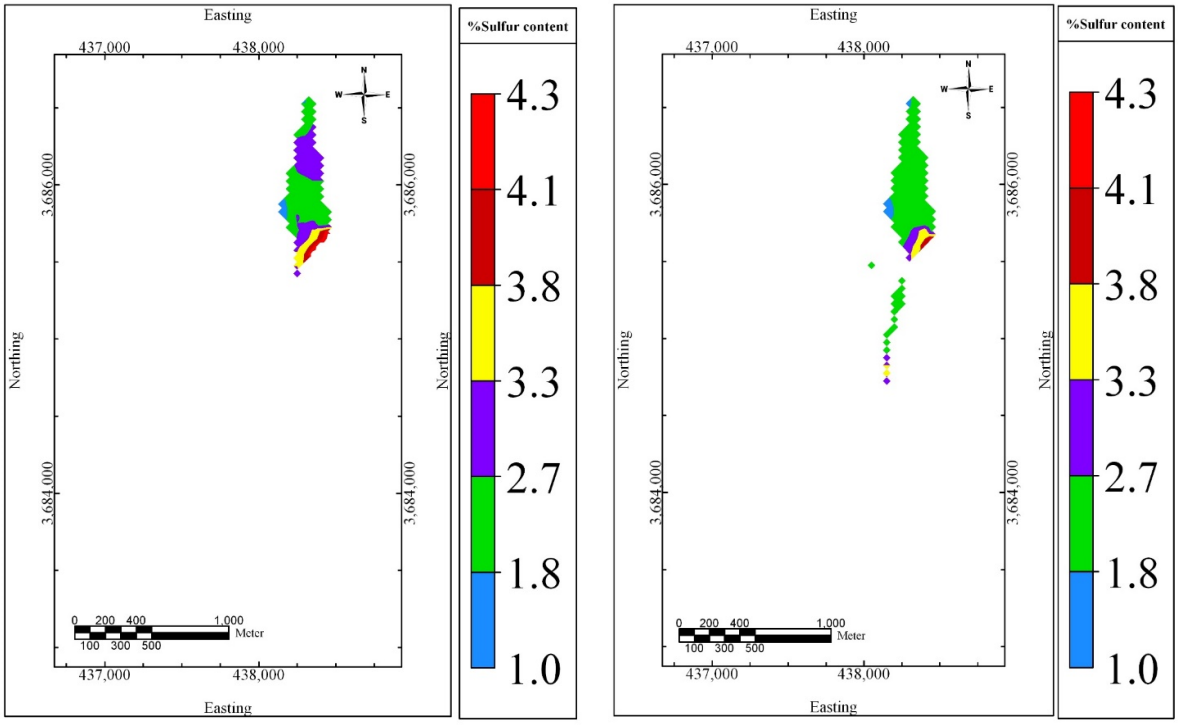

(c) (d)

Figure 12. Sulfur plan map in K7 seam (c- at 900 meters and d- at 1000 meters).

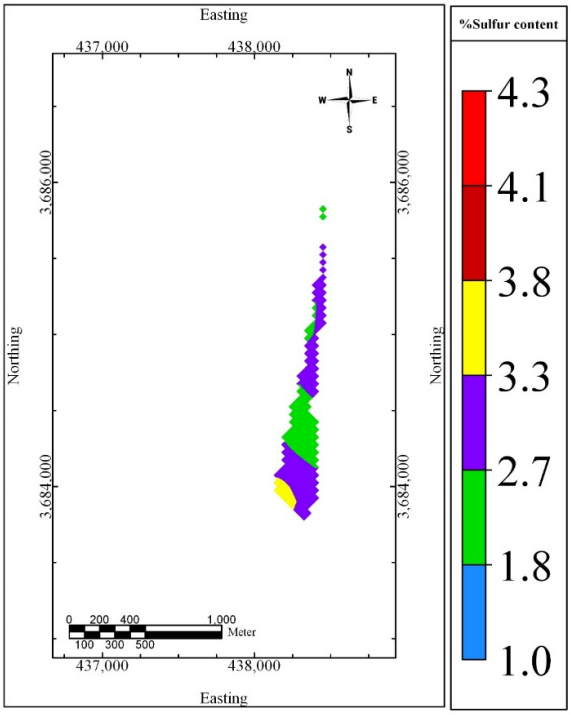

Figure 13. Sulfur plan map in K7 seam at 1100 meters.

The results show that in K1 seam low ash concentrations (Ash < 30.2%) at 755, 800, 900, 1000, and 1100 meters of depth are concentrated in most parts of the seam. The plans at different depths show that most parts of the K1 seam have concentrations less than 30.2%; only a small part in 755 meters of depth has moderate ash concentrations, whereas high (50.11%-72.4%) and very high (> 72.4%) ash concentrations are very limited in K1 seam (Figures 14, 15, and 16).

Low concentrations of ash in the K7 seam (Ash <33.1%) based on C-V fractal model are located at 755, 800, 900, and 1100 meters of depth in the northern, southern, and eastern parts of K7 seam but these concentrations are mostly found at the southeastern part of K7 seam at an depth of 1000 meters. According to the C-V model, moderate ash concentrations (33.1%-45.7%) at various depths are concentrated in the western part of K7 seam. Based on the C-V model, relatively high ash concentrations (45.7%-66.06%) are only found at 1000 meters of depth at the northwestern part of the seam. Traces of high (66.06%-85.1%) and very high (Ash > 85.1%); ash concentrations are not seen in plans at different depths in K7 seam, so they have limited frequency (Figures 17, 18, 19).

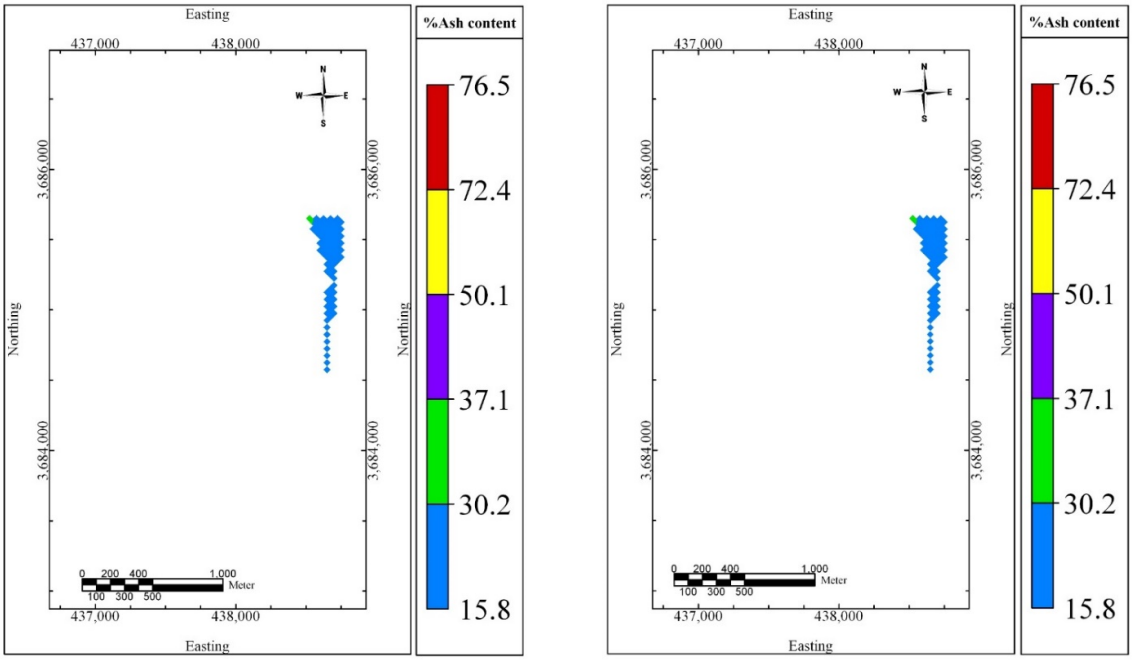

(a) (b)

Figure 14. Ash plan map in K1 seam (a- at 755 meters and b- at 800 meters).

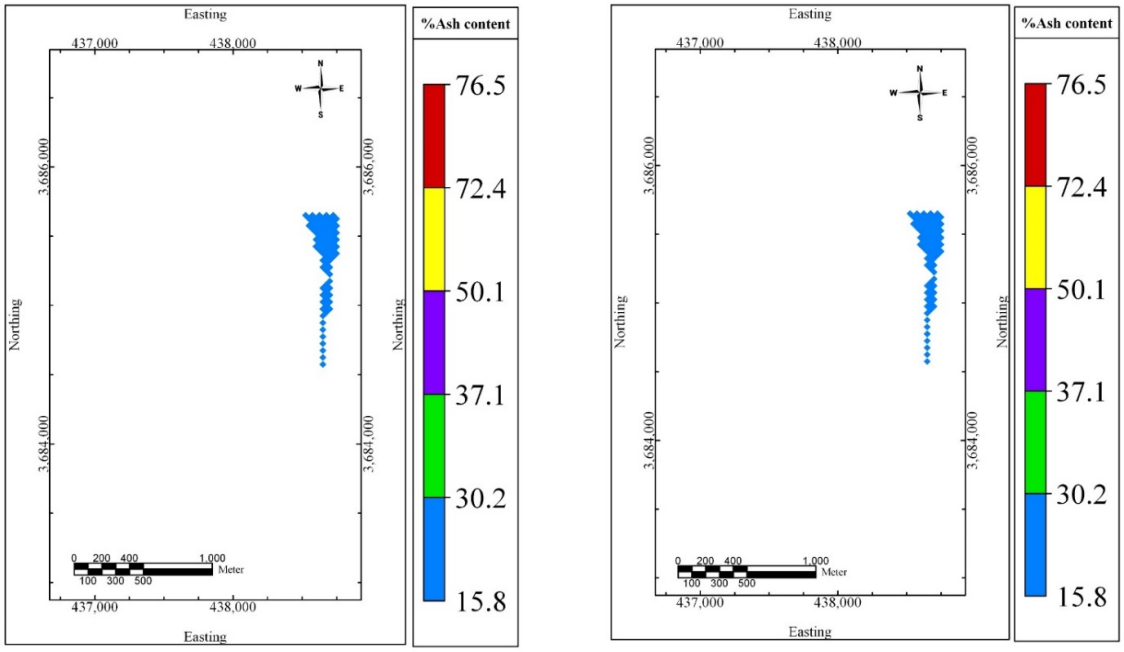

(c) (d)

Figure 15. Ash plan map in K1 seam (c- at 900 meters and d- at 1000 meters).

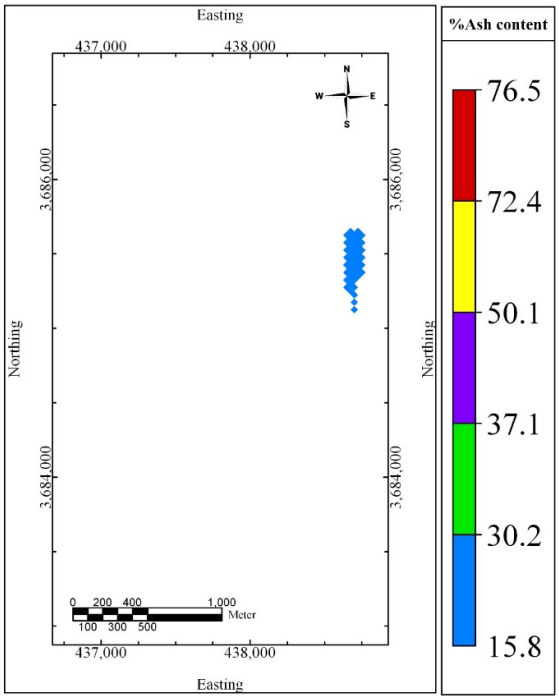

Figure 16. Ash plan map in K1 seam at 1100 meters.

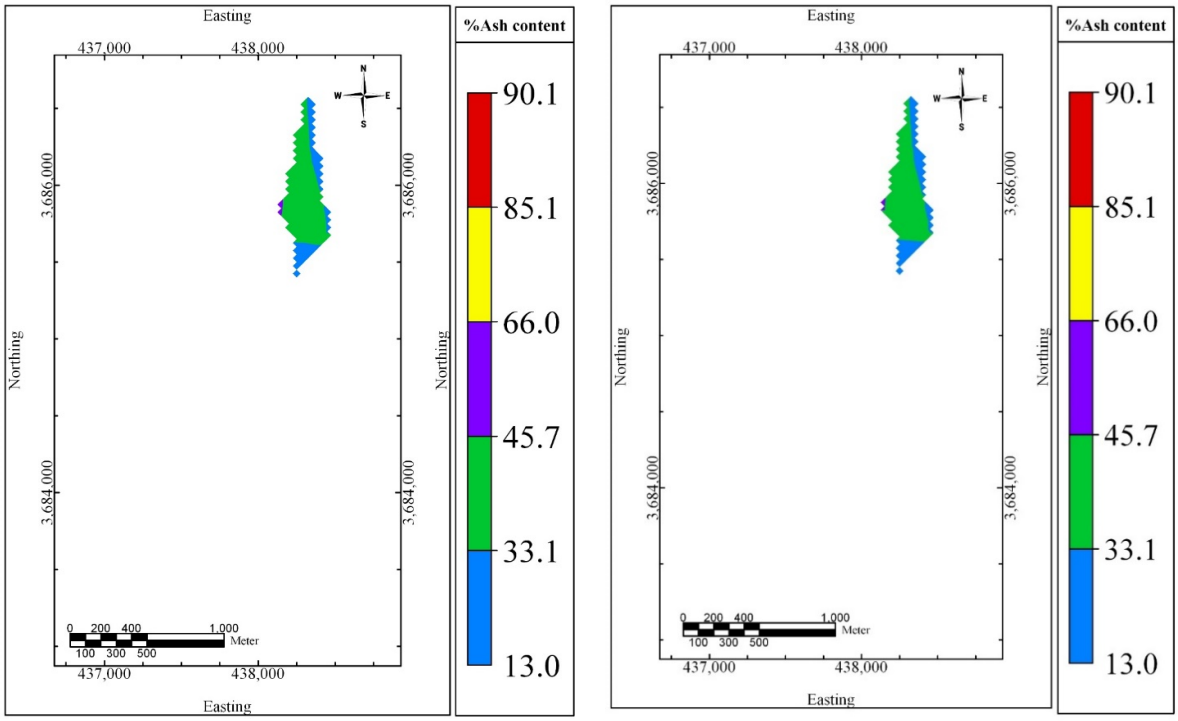

(a) **(b)**

Figure 17. Ash plan map in K7 seam (a- at 755 meters and b- at 800 meters).

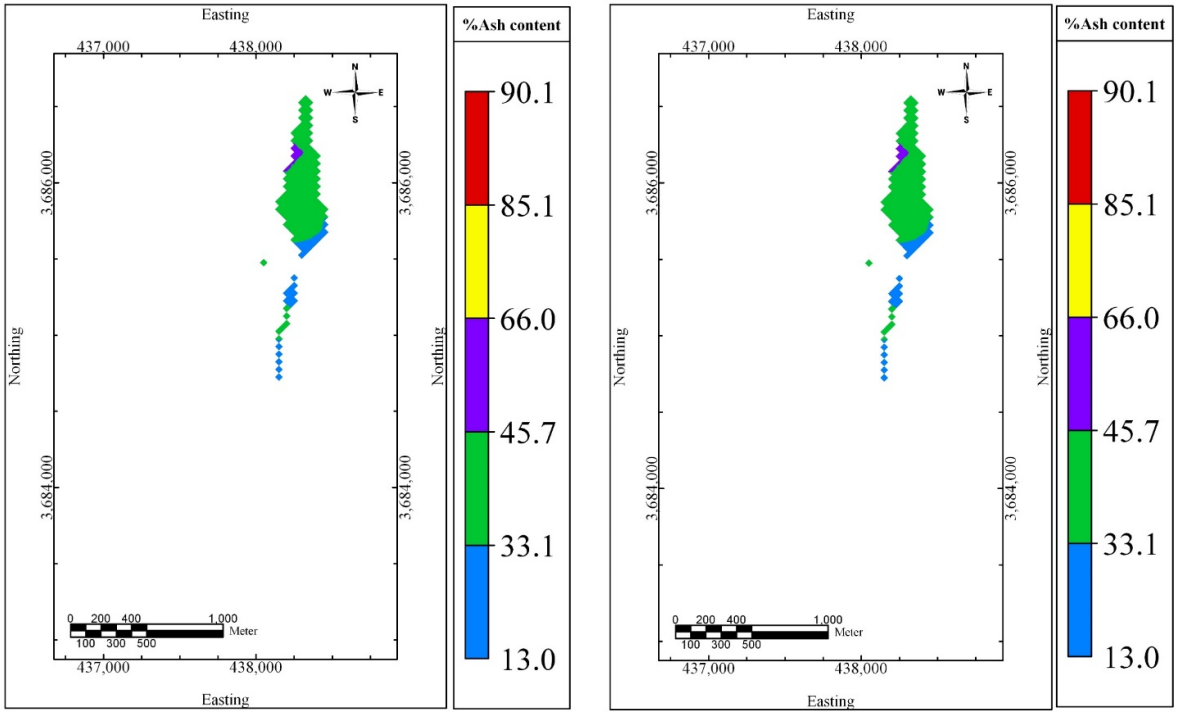

(c) (d)

Figure 18. Ash plan map in K7 seam (c- at 900 meters and d- at 1000 meters).

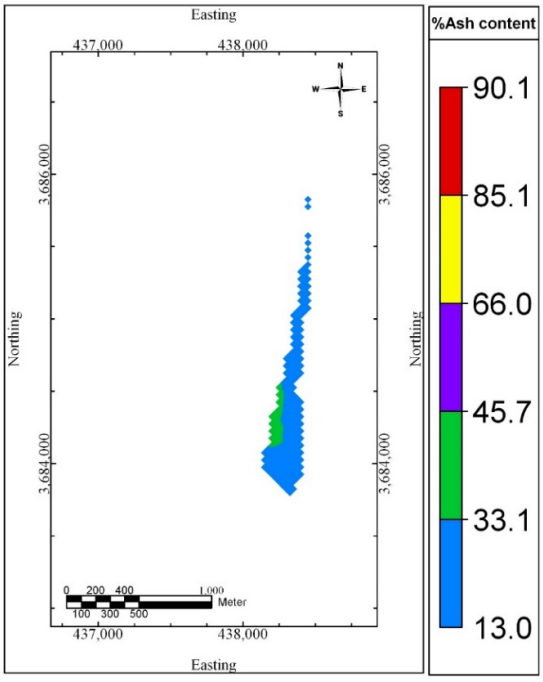

Figure 19. Ash plan map in K7 seam at 1100 meters.

The C-V fractal model can show various phases of carbonization. In the first phase, coal or ash content could be 45.7% for the K1 seam and over 37.1% for the K7 seam. This phase can be identified by the presence of coal ash and pyrite veins in the region. In this phase, coal has a high sulfur concentration, which exceeds 3.8% for both seams based on the fractal model. Based on the C-V fractal model, the main carbonization phase corresponds to sulfur and ash concentrations, respectively, below 4.46% and 37.1% for the K1 seam and below 1.8% and 33.1% for the K7 seam.

In this section, an attempt has been made to examine the compatibility of the zones obtained from the C-V fractal models and geological observations or data for this purpose. An analysis for calculating the spatial correlation or overlap between two paired models (e.g. geological and mathematical models such as fractal modeling or geostatistics) proposed by [74]. Thus a model with four overlapping conditions was produced for obtaining the number of voxels (efficiency of the paired geo-chemical distribution model) for all four overlap classes. The number of voxels overlapping between the two models are used for obtaining the overall accuracy (OA) and type-1 and 2 (TELL I and TELL II) errors. The four overlapping parameters (A, B, C, and D) for the sulfur and ash for two variables (C-V fractal models and geological data) of the K1 and K7 seams were defined and placed in the formulated logratio matrix to obtain OA, TELL I, and TELL II (Table 7).

OA and TELL I and TELL II correspond to the efficiency analysis of the relevant mineral zones. TELL I and TELL II error shows the difference between two sets of data (C-V fractal model zones and geological data) but TELL II error shows this difference better. The match between the C-V fractal model and the pyrite vein for both K1 and K7 coal seams were obtained using the logratio matrix (Figures 20 and 21).

Concentrations more than 3.8% and more than 40%, respectively, indicate pyrite vein and coal ash according to the Russian standard, so that number of samples with concentrations more and less than 3.8% and 45.7% for sulfur and ash, respectively, in K7 seam and the number of samples with concentrations more and less than 4.4% and 37.1% for sulfur and ash, respectively, in K1 seam that were obtained based on the C-V fractal graphs were used to calculate the parameters of A, B, C, and D.

In general, OA values greater than 0.5 indicate good correlation and more than 0.8 indicate very good correlation between the two models [70]. The OA values for high sulfur concentration in K1 and K7 seams and pyrite veins are 0.87 and 0.77, which show very good for K1 seam and good correlation between geological data and C-V fractal modeling (Tables 8 and 10). There are almost suitable values of OAs between ash coals and high ash populations derived via C–V fractal modeling; these values are 0.53 and 0.52 for the K7 and K1 seams, respectively (Tables 9 and 11).

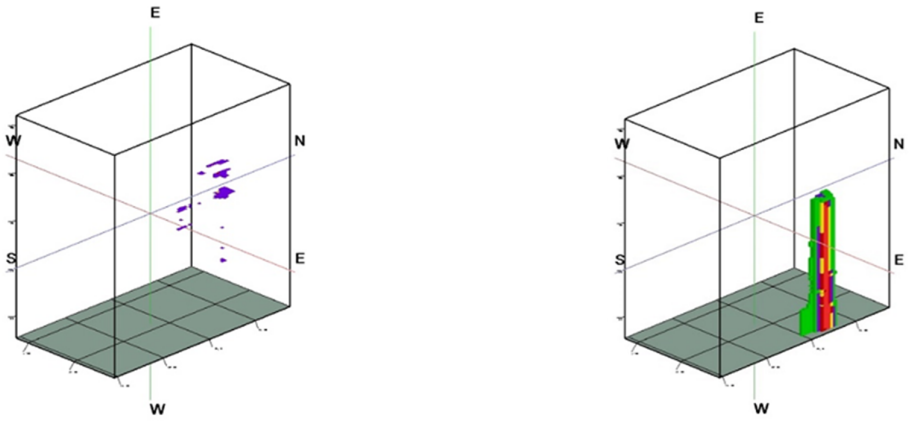

(a) **(b)**

Figure 20. a- Pyritic veins b- ash coals in the K1 seam.

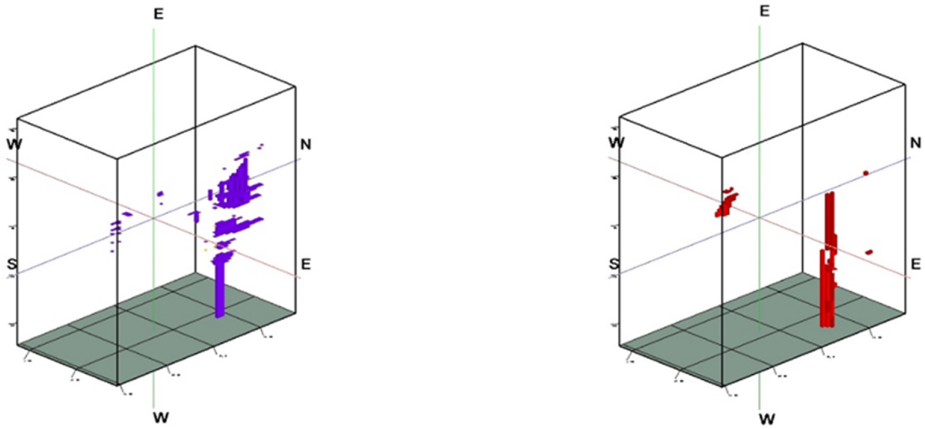

(a) (b)

Figure 21. a- Pyritic veins b- ash coals in the K7 seam.

Table 7. The overlap matrix that shows the results related to the fractal model and the geological model. A, B, C, and D parameters indicate numbers of voxels in overlaps between classes in the binary geological model and the binary results of the fractal models [74].

	Geological model	
	Inside zone	**Outside zone**
Fractal model	True positive (A)	False positive (B)
	True negative (C)	False negative (D)
	Type I error= C/(A+C)	Type II error = B/(B+D)
	Overall accuracy= (A+D)/(A+B+C+D)	

Table 8. Logratiomatrix for high sulfur content in K1 seam of North Kochakali coal deposit.

		Geological model	
		Inside zone	**Outside zone**
Fractal model	Inside zone > 4.4	2 (A)	12 (B)
	Outside zone < 4.4	8 (C)	132 (D)
		Type I error= 0.8	Type II error = 0.08
		Overall accuracy= 0.87	

Table 9. Logratio matrix for high ash content in K1 seam of the North Kochakali coal deposit.

		Geological model	
		Inside zone	**Outside zone**
Fractal model	Inside zone > 37.1	123 (A)	294 (B)
	Outside zone < 37.1	87 (C)	290 (D)
		Type I error= 0.4	Type II error = 0.5
		Overall accuracy= 0.52	

Table 10. Logratiomatrix for high sulfur content in K7 seam of North Kochakali coal deposit.

		Geological model	
		Inside zone	**Outside zone**
Fractal model	Inside zone > 3.8	4 (A)	19 (B)
	Outside zone < 3.8	16 (C)	115 (D)
		Type I error= 0.8	Type II error = 0.14
		Overall accuracy= 0.77	

Table 11. Logratio matrix for high ash content in K7 seam of the North Kochakali coal deposit.

		Geological model	
		Inside zone	**Outside zone**
Fractal model	Inside zone > 45.7	43 (A)	308 (B)
	Outside zone < 45.7	65 (C)	378 (D)
		Type I error= 0.6	Type II error = 0.44
		Overall accuracy= 0.53	

5. Conclusions

1. The results of this research work show that the C-V fractal model can be used as a suitable tool to evaluate the quality of different parts in the coal layer. C-V fractal models in the North Kochakali deposit show a good correlation with the Russian standard. According to log-log C-V graph, ash concentrations lees than 33.1% for the K7 seam and less than 37.1% for the K1 seam were chosen as appropriate ash concentrations for these seams, which correlate with Russian standard. Due to the high sulfur content in North Kochakali coal populations with very low sulfur content based on C-V fractal models were selected as appropriate sulfur concentrations for K1 and K7 seams, so concentrations less than 1.86% for K1 seam and concentrations less than 4.46 for K7 seam were considered as correct concentrations.
2. Based on C-V fractal graphs population with low ash content and population with very low sulfur content in all plans of K1 seam are located at southern part of this seam, so the southern part of K1 seam has the highest quality based on sulfur and ash concentrations. Population with very low sulfur content in K7 seam at all different depths is located at northern and northwest part of K7 seam, and population with low ash content in K7 seam in all different plans except 800- and 900-meters depth is located in north part of this seam, so the north part of K7 seam has the highest quality base on sulfur and ash concentrations.
3. Several plans show that the concentrations of sulfur and ash decreases towards the surface, and this decrease due to severe faulting in the North Kochakali area can be the result of the activity of the dip-slip faults in the area, which with their activity causes crushing and increase ash coal and also makes the area susceptible to fluid movement. The higher sulfur content in the K1 seam compared to K7 seam, considering that K1 seam in the Hojedk Formation is located in a deeper part than K7 seam, indicates the essence of the issue that sulfur-containing fluids penetrated more in the K1 seam during the Paleogene.
4. Open-pit or underground mining operations from high quality parts of the coal seams, which are obtained based on C-V fractal model and using sulfur, and ash concentrations will reduce environmental effects and side costs, in addition these parts also have a higher economic value but there are always challenges such as environmental conditions of study area, human errors, costs, equipment, and laboratory errors that can affect the research results. There are many valuable elements in coal, whose existence has been proven by many researchers. The existence of these elements can affect the overall quality of the coal seam as well as its economic value, which provide the basis for further research.

Acknowledgment

The authors would like to thank Ms. Zahra Aghaei from Falat Zarin Kimia for authorizing the access to the North-Kochakali drill cores and dataset.

References

[1]. Nouri, R., Jafari, M., Arian, M., Feizi, F., & Afzal, P. (2013a). Correlation between Cu mineralization and major faults using multifractal modelling in the Tarom area (NW Iran). *Geologica Carpathica, 64*(5), 409-416.

[2]. Nouri, R., Jafari, M.R., Arian, M., Feizi, F., & Afzal, P. (2013b). Prospection for Copper Mineralization with Contribution of Remote Sensing, Geochemical and Mineralographical Data in Abhar 1:100,000 Sheet, NW Iran. *Archives of Mining Sciences, 58*(4), 1071-1084.

[3]. Nouri, R. & Arian, M. (2017). Multifractal modeling of the gold mineralization in the Takab area (NW Iran). *Arabian Journal of Geosciences, 10*(5), 105.

[4]. Mansouri, E., Feizi, F., Jafari Rad, A., & Arian, M. (2017). A comparative analysis of index overlay and topsis (based on AHP weight) for Iron Skarn Mineral prospectivity mapping, a case study in Sarvian Area, Markazi Province, Iran. *Bulletin of the Mineral Research and Exploration, 155*, 147-160.

[5]. Mansouri, E., Feizi, F., Jafari Rad, A., & Arian, M. (2018). Remote-sensing data processing with the multivariate regression analysis method for iron mineral resource potential mapping: a case study in the Sarvian area, central Iran. *Solid Earth, 9*(2), 373-384.

[6]. Nabilou, M., Arian, M., Afzal, P., Adib, A., & Kazemi, A. (2018). Determination of relationship between basement faults and alteration zones in Bafq-

Esfordi region, central Iran. *Episodes Journal of International Geoscience, 41*(3), 143-159.

[7]. Arian, M. (2012). Clustering of Diapiric Provinces in the Central Iran Basin. *Carbonates and Evaporites, 27*(1), 9-18.

[8]. Arian, M., Bagha, N., Khavari, R., & Noroozpour, H. (2012). Seismic Sources and Neo-Tectonics of Tehran Area (North Iran). *Indian Journal of Science and Technology, 5*(3), 2379-2383.

[9]. Arian, M. & Aram, Z. (2014). Relative Tectonic Activity Classification in the Kermanshah Area, Western Iran. *Solid Earth, 5*(2), 1277-1291.

[10]. Arian, M. (2015). Seismotectonic-Geologic Hazards Zoning of Iran. *Earth Sciences Research Journal, 19*(1), 7-13.

[11]. Ehsani, J. & Arian, M. (2015). Quantitative Analysis of Relative Tectonic Activity in the Jarahi-Hendijan Basin Area, Zagros Iran. *Geosciences Journal, 19*(4), 1-15.

[12]. Aram, Z. & Arian, M. (2016). Active Tectonics of the Gharasu River Basin in Zagros, Iran, Investigated by Calculation of Geomorphic Indices and Group Decision using Analytic Hierarchy Process (AHP) Software. *Episodes, 39*(1), 39-44.

[13]. Razaghian, G., Beitollahi, A., Pourkermani, M., & Arian, M. (2018). Determining seismotectonic provinces based on seismicity coefficients in Iran. *Journal of Geodynamics, 119*(20), 29-46.

[14]. Taesiri, V., Pourkermani, M., Sorbi, A., Almasian, M., & Arian, M. (2020). Morphotectonics of Alborz Province (Iran): A Case Study using GIS Method. *Geotectonics, 54*(5), 691-704.

[15]. Khavari, R., Arian, M., & Ghorashi, M. (2009). Neotectonics of the South Central Alborz Drainage Basin, in NW Tehran, N Iran. *Journal of Applied Sciences, 9*(23), 4115-4126.

[16]. Fürsich, F.T., Wilmsen, M., Seyed-Emami, K., & Majidifard, M.R. (2009). Lithostratigraphy of the Upper Triassic–Middle Jurassic Shemshak Group of Northern Iran. In South Caspian to Central Iran Basins. Geological Society of London*, Special Publication, 312*(1), 129–60.

[17]. Salehi, M. A., Wilmsen, M., Zamanian, E., Baniasad, A., & Heubeck, C. (2022). Depositional and thermal history of a continental, coal-bearing Middle Jurassic succession from Iran: Hojedk Formation, northern Tabas Block. *Geological Magazine, 160*(2), 235-259.

[18]. Demirbas, A. & Karslioglu, S. (2004). Removal of organic sulfur from coal by wheat straw ash and potassium ferric hexacyanoferrat (II). *Energy Exploration & Exploitation, 22*(6), 429-439.

[19]. Ayhan, F.D., Abakay, H., & Saydut, A. (2005). Desulfurization and deashing of Hazro coal via a flotation method. *Energy & Fuels, 19*(3), 1003-1007.

[20]. Duz, M.Z., Tonbul, Y., Baysal, A., Akba, O., Saydut, A., & Hamamci, C. (2005). Pyrolysis kinetics and chemical composition of Hazro coal according to the particle size. *Journal of Thermal Analysis and Calorimetry, 81* (2), 395-398.

[21]. Erdogan, S., Baysal A., Akba O., & Hamamci C. (2007). Interaction of metals with humic acid isolated from oxidized coal. *Polish Journal of Environmental Studie, 16*(5), 671-675.

[22]. Zhao, C.L. & Sun Y.Z. (2008). Rare earth elements of coal seam 5 from Gequan Mine, Xingtai Coalfield. *World Journal of Engineering, 5*(1), 90-94.

[23]. Zhao C.L., Qin S.J., Yang Y.C., Li Y.H., & Lin M.Y. (2009). Concentration of gallium in the Permo-Carboniferous coals of China. *Energy Exploration & Exploitation, 27*(5), 333-343.

[24]. Shukla, A., Prasad, A.K., Mishra, S., Vinod, A., & Varma, A.K. (2023). Rapid Estimation of Sulfur Contentin High-Ash Indian Coal using Mid-Infrared FT-IR Data. *Minerals, 13*(5), 1-20.

[25]. Calkins, W.H. (1994). The Chemical Forms of Sulfur in Coal. A Review. *Fuel 1994, 73*(4), 475–484.

[26]. GoldsWorthy, P., Eyre, D.J., & On, E. (2013). Value-in-Use (VIU) Assessment for Thermal and Metallurgical Coal. In The Coal Handbook: Towards Cleaner Production, Elsevier, Amsterdam, 496 P.

[27]. Zheng, B., Ding, Z., Huang, R., Zhu, J., Yu, X., Wang, A., Zhou, D., Mao, D., & Su, H. (1999). Issues of health and disease relating to coal use in Southwest China. *International Journal of Coal Geology, 40*(2-3), 119−132.

[28]. Wu, M., Shen, J., Qin, Y., Qin. Yo., Wang, X., & Zhu. S. (2022). Method of Identifying Total Sulfur Content in Coal: Geochemical and Geophysical Logging Data from the Upper Paleozoic in North China. *ACS Omega*, 7 (49), 45-56.

[29]. Yang, X., Ingham, D., Ma, L., Srinivasan, N., & Pourkashanian, M. (2017). Ash Deposition Propensity of Coals/Blends Combustion in Boilers: A Modeling Analysis based on Multi-Slagging Routes. Proc. *Combust. Inst, 36*(3), 41–50.

[30]. Yazdi, M., & Golzar, H. (2012). Geochemical properties and environmental impacts of the Mazino coal. *European Chemical Bulletin, 1*(5), 125-129.

[31]. Mandelbrot, B.B. (1983). The Fractal Geometry of Nature. *Freeman*, San Fransisco, 468 P.

[32]. Cheng, Q., Agterberg, F.P., & Ballantyne, S.B. (1994). The separation of geochemical anomalies from background by fractal methods. *Journal of Geochemical Exploration, 51*(2), 109–130.

[33]. Agterberg, F.P., Cheng, Q., Brown, A., & Good, D. (1996). Multifractal modeling of fractures inthe Lac du Bonnet Batholith, Manitoba. *Computers & Geosciences, 22*(5), 497–507.

[34]. Costa, J.F. (1997). Development in Recoverable Reserves and Ore Body Modeling, *WH Bryan Mining Geology Research Centre*, University of Queensland, 333 P.

[35]. Turcotte, D.L. (1997). Fractals and Chaos in Geology and Geophysics, Cambridge Univ Press, Cambridge, 416 P.

[36]. Costa, J.F. & Dimitrakopoulos, R. (1998). A conditional fractal (fBm) simulation approach for orebody modelling. *International journal of surface mining, reclamation and environment, 12*(4), 197–202.

[37]. Li, C., Ma, T., & Shi, J. (2003). Application of a fractal method relating concentrations and distances for separation of geochemical anomalies from background. *Journal of Geochemical Exploration, 77*(2), 167–175.

[38]. Cheng, Q. (2007). Mapping singularities with stream sediment geochemical data for prediction of undiscovered mineral deposits in Gejiu, Yunnan Province. *Ore Geology Reviews, 32*(2), 314‑324.

[39]. Zuo, R., Cheng, Q., & Xia, Q. (2009). Application of fractal models to characterization of vertical

distribution of geochemical element concentration. *Journal of Geochemical Exploration, 102*(1), 37–43.

[40]. Afzal, P., FadakarAlghalandis, Y., Khakzad, A., Moarefvand, P., & Rashidnejad Omran, N. (2011). Delineation of mineralization zones in porphyry Cu deposits by fractal concentration–volume modeling. *Journal of Geochemical Exploration, 6*(7): 220–232.

[41]. Daneshvar Saein, L., Rasa, I., Rashidnejad Omran, N., Moarefvand, P., Afzal, P., & Sadeghi, B. (2012). Application of number–size (N–S) fractal model to quantify of the vertical distributions of Cu and Mo in Nowchun porphyry deposit (Kerman, SE Iran). *Archives of Mining Sciences, 58*(1), 89–105.

[42]. Zuo, R., Carranza, E.J.M., & Cheng, Q. (2012). Fractal/multifractal modelling of geochemical exploration data *Journal of Geochemical Exploration*, 122 (12), 33-41.

[43]. Afzal, P., Dadashzadeh Ahari, H., RashidnejadOmran, N., & Aliyari, F. (2013). Delineation of gold mineralized zones using concentration–volume fractal model in Qolqoleh gold deposit, NW Iran. *Ore Geology Reviews. 55*(6), 125–133.

[44]. Yasrebi, A.B., Afzal, P., Wetherelt, A., Foster, P.J., & Esfahanipour, R. (2013). Correlation between geology and concentration–volume fractal models: significance for Cu and Mo mineralised zones separation in Kahang porphyry deposit, Central Iran. *Geologica Carpathica, 64*(2), 153–163.

[45]. Zuo, R., Xia, Q., & Wang, H., 2013. Compositional data analysis in the study of integratedgeochemical anomalies associated with mineralization. *Applied Geochemistry, 28*(12), 202–221.

[46]. Cheng, Q.M. (1995). The perimeter–area fractal model and its application to geology. *Mathematical Geosciences, 27*(6), 69–82.

[47]. Afzal, p., Alhoseini, S.H., Tokhmechi, b., Kaveh Ahangaran, D., Yasrebi, A.B., Madani, N., & Wetherelt, A. (2014). Outlining of high quality coking coal by concentration–volume fractal model and turning bands simulation in East-Parvadeh coal deposit, Central Iran. *International Journal of Coal Geology, 127*, 88–99.

[48]. Cheng, Q., Xu, Y., & Grunsky, E. (1999). Integrated spatial and spectral analysis for geochemical anomaly separation. In: Lippard, S.J., Naess, A., Sinding-Larsen, R. (Eds.), *Proc of the Conference of the International Association for Mathematical Geology, 1*, 87–92.

[49]. Sadeghi, B., Moarefvand, P., Afzal, P., Yasrebi, A.B., & Daneshvar Saein, L. (2012). Application of fractal models to outline mineralized zones in the Zaghia iron ore deposit, Central Iran. *Journal of Geochemical Exploration, 122*(10), 9–19.

[50]. Afzal, P. & Hassanpour, Sh. (2013). Application of concentration–number (C–N) multifractal modeling for geochemical anomaly separation in Haftcheshmeh porphyry system,NW Iran. *Arabian Journal of Geosciences, 6*(3), 957–970.

[51]. Afzal, P., Mirzaei, M., Yousefi, M., Adib, A., Khalajmasoumi, M., Zia Zarifi, A., Foster, P., & Yasrebi, A. (2016). Delineation of geochemical anomalies based on stream sediment data utilizing fractal modeling and staged factor analysis. *Journal of African Earth Sciences, 119*, 139–149.

[52]. Mahdiyanfar, H. & Seyedrahimi Niaraq, M. (2023). Integration of Fractal and Multivariate Principal Component Models for Separating Pb-Zn Mineral Contaminated Areas. *Journal of Mining and Environment (JME), 14*(3), 1019-1035.

[53]. Soltani, F., Afzal, P., & Asghari, O. (2014). Delineation of alteration zones based on Sequential Gaussian Simulation and concentration–volume fractal modeling in the hypogene zone of Sungun copper deposit, NW Iran. *Journal of Geochemical Exploration, 140*, 64-76.

[54]. Afzal, P., Yusefi, M., Mirzaie, M., Ghadiri-Sufi, E., Ghasemzadeh, S., & Daneshvar Saein, L. (2019). Delineation of podiform-type chromite mineralization using geochemical mineralization prospectivity index and staged factor analysis in Balvard area (SE Iran). *Journal of Mining and Environment, 10*(3), 705-715.

[55]. Kianersi, A., Adib, A., & Afzal, P. (2021). Detection of Effective Porosity and Permeability Zoning

in an Iranian OilField Using Fractal Modeling. *International Journal of Mining and Geo-Engineering, 55*(1), 49-58.

[56]. Zissimos, A. M., Cohen, D. R., Christoforou, I. C., Sadeghi, B., & Rutherford, N. F. (2021). Controls on soil geochemistry fractal characteristics in Lemesos (Limassol), Cyprus. *Journal of Geochemical Exploration, 220*(29), 162-172.

[57]. Kianoush, P., Mohammadi, G., Hosseini, S. A., Keshavazr Faraj Khah, N., & Afzal, P. (2022). Compressional and Shear Interval Velocity Modeling to Determine Formation Pressures in an Oilfield of SW Iran. *Journal of Mining and Environment, 13*(3), 851-873.

[58]. Mahdizadeh, M., Afzal, P., Eftekhari, M., & Ahangari, K. (2022). Geomechanical zonation using multivariate fractal modeling in Chadormalu iron mine, Central Iran. *Bulletin of Engineering Geology and the Environment, 81*(1), 59.

[59]. Mirzaei, M., Adib, A., Afzal, P., Rahemi, E., & Mohammadi, G. (2022). Separation of geological ore and gangues zones based on multivariate fractal modeling in Jalal Abad iron ore deposit, Central Iran. Advanced *Applied Geology, 12*(3), 573-588.

[60]. Sim, B.L., Agterberg, F.P. & Beaudry, C. (1999). Determining the cutoff between background and relative base metal contamination levels using multifractal methods. *Computers & Geosciences, 25*(9), 1023–1041.

[61]. Salarian,S., Asghari, O.,Abedi, M., & Alilou, S.K. (2019). Geostatistical and multi-fractal modeling of geological and geophysical characteristics in Ghalandar Skarn-Porphyry Cu Deposit, Iran. *Journal of Mining and Environment (JME), 10*(4), 1061- 1081.

[62]. Khalajmasoumi, M., Lotfi, M., Afzal, P., Sadeghi, B., Memar Kochebagh, A., Khakzad, A., & Ziazarifi, A. (2015). Delineation of the radioactive elements based on the radiometric data using concentration–area fractal method in the Saghand area, Central Iran. *Arabian Journal of Geosciences, 8(8)*, 6047–6062.

[63]. Seyedrahimi Niaraq, M., & Hekmatnejad, A. (2020). The efficiency and accuracy of probability diagram, spatial statistic and fractal methods in the identification of shear zone gold mineralization: a case study of the Saqqez gold ore district, NW Iran. *Acta Geochim, 40*(1), 78-88.

[64]. Yasrebi, A.B., Hezarkhani, A., & Afzal, P. (2017). Application of Present Value-Volume (PV-V) and NPV-Cumulative Total Ore (NPV-CTO) fractal modelling for mining strategy selection. *Resources Policy, 53*, 384-393.

[65]. Pazand, K. (2015). Rare earth element geochemistry of coals from the Mazino Coal Mine, Tabas Coalfield, Iran. *Arabian Journal of Geosciences, 8*(12), 59–69.

[66]. AliMolaei, M. & Aminzadeh, A. (2019). Geochemical properties of major and rare earth elements in the South Kouchek-Ali Coal Mine, Tabas. *Journal of Economic Geology, 11*(2), 321 – 337.

[67]. Aghanabati, S.A. (2004). Geology of Iran. Tehran, Geological Survey of Iran (in Persian), 586 P.

[68]. Mohamadi, A. (2014). Thermal Coal Project-Exploration in the South Kouchek-Ali Coal Mine, Tabas. Kavesh Kansar Engineering Company, Tehran, 230 P.

[69]. Seyed-Emami, K., Schairer, G., Fürsich, F.T., Wilmsen, M., & Majidifard, M.R. (2000). First record of ammonites from the Badamu Formation at the Shotori Mountains (CentralIran). *Eclogae Geologiae Helvetiae, 93*(2) 257‑263

[70]. Geological Suvey of Iran, Iran DEM.

[71]. Geological Suvey of Iran, 1:100000 Robatkhan map.

[72]. Wood, G.H. & Kehn, M. (1976). Coal Resource Classification System of U.S. Geological Survey, USA

[73]. Skochinsky, A. & Komarov, V. (1996). Mine ventilation, Mir publishers, Moscow, Russia.

[74]. Carranza, E.J.M. (2011). Analysis and mapping of geochemical anomalies using log ratiotransformedstream sediment data with censored values. *Journal of Geochemical Exploration, 110*(2), 167–185.

تعیین بخش‌های باکیفیت زغالسنگ با استفاده از مدل فرکتالی عیار-حجم در کانسار زغالسنگ کوچکعلی شمالی، ایران مرکزی

مجتبی بازرگانی گلشن[۱]، مهران آرین[۱*]، پیمان افضل[۲]، لی‌لی دانشور صایین[۳] و محسن آل‌علی[۱]

۱- گروه علوم زمین، واحد علوم و تحقیقات، دانشگاه آزاد اسلامی، تهران، ایران
۲- گروه مهندسی نفت و معدن، واحد تهران جنوب، دانشگاه آزاد اسلامی، تهران، ایران
۳- گروه زمین شناسی، دانشگاه پیام نور، صندوق پستی ۳۶۹۷-۱۹۳۹۵، تهران، ایران

ارسال ۲۰۲۳/۰۸/۰۷، پذیرش ۲۰۲۳/۱۱/۰۲

* نویسنده مسئول مکاتبات: mehranarian@yahoo.com

چکیده:

هدف استفاده از مدل فرکتالی عیار- حجم برای شناسایی بخش‌های با کیفیت بالا لایه‌های زغالسنگ براساس عیار گوگرد و خاکستر است. در لایه‌های زغالسنگ K1 و K7 در کانسار زغالسنگ کوچکعلی شمالی، ۵ و ۶ فراوانی مختلف خاکستر و گوگرد براساس نتایج بدست آمد. براساس این مدل به‌ترتیب عیارهای گوگرد و خاکستر پایین تر از ۱.۸۱ و ۳۳.۱ درصد برای لایه K7، و عیارهای گوگرد و خاکستر پایین تر از ۴.۴۶ و ۳۷.۱ درصد برای لایه K1، براساس استاندارد روسیه برای خاکستر و محتوای بالای گوگرد زغالسنگ کوچکعلی شمالی به‌عنوان مقادیر مناسب در نظر گرفته شد. به‌منظور شناسایی بخش‌های باکیفیت لایه‌های زغال سنگ K1 و K7 از پلان هایی در اعماق مختلف بر اساس مدل فرکتالی عیار- حجم استفاده شد. پلان‌ها در اعماق مختلف نشان می‌دهد که قسمت جنوبی لایه K1 و قسمت شمالی لایه K7 دارای بالاترین کیفیت براساس عیارهای گوگرد و خاکستر می‌باشد که باید در عملیات استخراج در نظر گرفته شود. از ماتریس لوگرشیو به‌منظور مقایسه نتایج مدل فرکتالی عیار- حجم با داده‌های زمین شناسی رگه‌های پیریت و خاکستر زغالسنگ استفاده شد. این ماتریس نشان می‌دهد که میزان گوگرد بالای ۳.۸ درصد برای لایه K7 و بالای ۴.۴۱ درصد برای لایه K1 به‌ترتیب با رگه‌های پیریتی داده‌های زمین شناسی همبستگی خوب و بسیار خوبی دارند. مقادیر دقت کلی خوبی در ارتباط بین بخش‌های لایه با عیار خاکستر بالای ۳۷.۱ و ۴۵.۷ درصد به ترتیب برای لایه‌های K1 و K7، و خاکستر زغالسنگ بدست آمده از داده‌های زمین شناسی وجود دارد.

کلمات کلیدی: مدل فرکتالی عیار – حجم، زغالسنگ، کوچکعلی شمالی، ماتریس لوگرشیو، ایران مرکزی.